JOURNAL OF BACTERIOLOGY, May 2005, p. 3238–3248 Vol. 187, No. 9
0021-9193/05/$08.00+0 doi:10.1128/JB.187.9.3238–3248.2005

Molecular Determinants for PspA-Mediated Repression of the AAA Transcriptional Activator PspF

Sarah Elderkin,† Patricia Bordes, Susan Jones,‡ Mathieu Rappas, and Martin Buck*

Imperial College London, Department of Biological Sciences, Sir Alexander Fleming Building, South Kensington Campus, London SW7 2AZ, United Kingdom

Received 20 October 2004/Accepted 29 January 2005

The *Escherichia coli* phage shock protein system (*pspABCDE* operon and *pspG* gene) is induced by numerous stresses related to the membrane integrity state. Transcription of the *psp* genes requires the RNA polymerase containing the σ^{54} subunit and the AAA transcriptional activator PspF. PspF belongs to an atypical class of σ^{54} AAA activators in that it lacks an N-terminal regulatory domain and is instead negatively regulated by another regulatory protein, PspA. PspA therefore represses its own expression. The PspA protein is distributed between the cytoplasm and the inner membrane fraction. In addition to its transcriptional inhibitory role, PspA assists maintenance of the proton motive force and protein export. Several lines of in vitro evidence indicate that PspA-PspF interactions inhibit the ATPase activity of PspF, resulting in the inhibition of PspF-dependent gene expression. In this study, we characterize sequences within PspA and PspF crucial for the negative effect of PspA upon PspF. Using a protein fragmentation approach, we show that the integrity of the three putative N-terminal α-helical domains of PspA is crucial for the role of PspA as a negative regulator of PspF. A bacterial two-hybrid system allowed us to provide clear evidence for an interaction in *E. coli* between PspA and PspF in vivo, which strongly suggests that PspA-directed inhibition of PspF occurs via an inhibitory complex. Finally, we identify a single PspF residue that is a binding determinant for PspA.

Bacterial cell adaptation to changes in membrane integrity is crucial for their survival. One response to extracytoplasmic stress involves the phage *s*hock protein (Psp) system that is highly conserved in several gram-negative bacteria, including some pathogens. The *Escherichia coli psp* locus is made up of (i) two divergently transcribed cistrons, *pspABCDE* and *pspF*, and (ii) the newly identified *pspG* gene (22, 35). The Psp response is induced by the mislocalization of some outer membrane proteins, including secretins (38, 40); by mutations that cause secretion defects (16, 26, 27); and by a number of more general stresses, such as extreme heat and osmotic and ethanol shock (40). A common event resulting from all of these inducing conditions may be dissipation of the proton motive force (PMF). The PMF is important to achieve various membrane-mediated processes, such as protein translocation across the membrane and flagellar motor rotation (21, 43). Several lines of evidence suggest that PspA helps to sustain the PMF across the plasma membrane (31). Interestingly, the *psp* genes appear to be involved in bacterial infectious processes, since the Psp system is essential for the virulence of *Yersinia enterocolitica* (14, 15) and the *psp* genes are among the most highly upregulated genes in *Salmonella enterica* serovar Typhimurium during macrophage infection (20). Further, the *psp* operon is also upregulated during swarming in *S. enterica* serovar Typhimurium (48) and during biofilm formation in *E. coli* (3).

In *E. coli*, *pspA* and *pspG* promoter activities are dependent on the σ^{54} sigma factor of RNA polymerase (RNAP) (7, 35) and the σ^{54}-RNAP activator protein PspF (28). σ^{54} activators belong to the AAA (ATPases associated with various cellular activities) superfamily (42, 46, 53). Transcription initiation by σ^{54}-RNAP is strictly dependent on AAA activators, such as PspF (8). σ^{54} AAA activators typically bind to upstream activating sequences located upstream of the transcription start site and contact the σ^{54}-RNAP closed complex via DNA loop formation (51). σ^{54} AAA activators are macromolecular machines that convert the energy derived from ATP hydrolysis to a mechanical force, which is used to stimulate the isomerization of preformed σ^{54}-RNAP closed promoter complexes to open ones (9, 23). Their unifying structural feature is that they form ring-shaped higher-order oligomers required for ATPase activity, as the catalytic site lies at the interface between two adjacent protomers (46, 53). Although the exact oligomeric state of AAA activators is not clear, it has been established that one active form of the AAA domain of PspF is a hexameric ring (45, 46, 53).

AAA activators of the σ^{54}-RNAP are modular proteins, typically consisting of three functional domains (47): (i) a σ^{54}-interacting domain, the AAA domain, which is primarily responsible for ATP hydrolysis, self-association, and transcription activation (5, 12, 33, 46, 49, 53); (ii) an enhancer DNA-binding domain (DBD), usually located at the C-terminal end of the activator protein (51); and (iii) regulatory domains typically present in the N-terminal region of the protein, controlling the activity of the AAA activator in response to specific environmental cues (47). PspF belongs to an atypical class of

* Corresponding author. Mailing address: Imperial College London, Department of Biological Sciences, Sir Alexander Fleming Building, South Kensington Campus, London SW7 2AZ, United Kingdom. Phone: 44 207 594 5442. Fax: 44 207 594 5419. E-mail: m.buck@imperial.ac.uk.

† Present address: MRC Clinical Sciences Centre, Hammersmith Hospital Campus, London W12 0NN, United Kingdom.

‡ Present address: Nature Reviews Journals, Porters South, London N1 9XW, United Kingdom.

TABLE 1. Plasmids and bacterial strains

Plasmid or strain	Description	Reference
Plasmids		
pBAD18-Cm	Expression vector (pBAD); Cm^r	24
pAPT110	Expression vector (*lacUV5* promoter); Km^r	44
pGEMT-easy	Cloning vector; Ap^r	Promega
pET28b+	Expression vector (T7 promoter); Km^r	Novagen
pSLE18A	*E. coli pspA* gene in pET28b+	19
pPB9	*E. coli pspA* gene in pAPT110	This study
pSLE40	*E. coli pspF* gene in pET28b+	19
pSLE40-W56A	*E. coli pspFW56A* gene in pET28b+	This study
pPB8-WT	*E. coli pspF* gene in pBAD18-Cm	This study
pPB8-W56A	*E. coli pspFW56A* gene in pBAD18-Cm	This study
pPB1	*E. coli* $pspF_{1-275}$ gene in pET28b+	5
pPB1-W56A	*E. coli* $pspF_{1-275}$ *W56A* gene in pET28b+	This study
pSLEPspA1-186	*E. coli pspA1-186* gene in pET28b+	This study
pSLEPspA1-110	*E. coli pspA1-110* gene in pET28b+	This study
pSLEPspA110-222	*E. coli pspA110-222* gene in pET28b+	This study
pSLEPspA67-222	*E. coli pspA67-222* gene in pET28b+	This study
pSLEPspA67-186	*E. coli pspA67-186* gene in pET28b+	This study
pSR658	Wild-type $LexA_{DBD}$ fusion vector; Tc^r	17
pSR659	Mutant $LexA_{DBD}$ fusion vector; Ap^r	17
Strains		
MC1061	Cloning strain	11
MVA4	MC1061 Φ(*pspA-lac*)	Gift from G. Jovanovic
SU101	Homodimerization reporter strain (Wild-type *sulA*, promoter *lex*A operator op^+/op^+, fused to *lac*Z)	17
SU202	Heterodimerization reporter strain (Mutant *sulA* promoter, *lex*A operator $op408^+/op^+$, fused to *lac*Z)	17
MG1655 Δ*pspA*	In-frame deletion of *pspA*	35

AAA activators that lack a regulatory domain but are regulated by direct in *trans* interactions with other regulatory proteins. PspF is negatively regulated by PspA (18, 19, 40), and hence, PspA has at least two roles: (i) helping the bacterial cells to cope with alterations of the cell membrane and (ii) repressing its own transcription and that of *psp* genes.

PspA is a peripheral inner membrane protein that exists in a membrane-attached and a soluble form (6, 30). The molecular mode of action for PspA as a negative regulator of PspF remains poorly understood. Previous studies showed that PspA forms a complex with the AAA domain of PspF in vitro and that PspA inhibits PspF ATPase activity, possibly by preventing nucleotide access to the active site or by inhibiting formation of the correct oligomeric form (19, 25). PspA shows no sequence similarities with the regulatory domains of other AAA activators, but it has a homologue found in photosynthetic bacteria and plant chloroplasts, VIPP1, which is involved in thylakoid biogenesis (32, 50).

Here, we characterize sequences within PspA and PspF that are crucial for PspA-mediated inhibition of PspF. We conducted protein fragmentation studies to obtain partial sequences of PspA that retained the ability to inhibit PspF-dependent gene activation in vivo and in vitro. The requirement for the integrity of a large N-terminal part of PspA for its activity was established. In addition, based on the crystal structure of the AAA activator NtrC1 from *Aquifex aeolicus* (34), we derived a theoretical model of a hexameric ring of the AAA domain of PspF ($PspF_{1-275}$). Using this model, we identified a PspF-specific residue (W56) exposed at the surface of the PspF hexamer and show that it is a determinant for binding PspA.

MATERIALS AND METHODS

Bacterial strains and culture conditions. The bacterial strains and plasmids used in this study are listed in Table 1. Cells were grown aerobically at 37°C in LB medium. When required, ampicillin, kanamycin, chloramphenicol, and tetracycline were used at concentrations of 100, 50, 30, and 10 μg/ml, respectively.

DNA manipulations. pSLE18A was the template to amplify DNA encoding PspA fragments using appropriate primers for $PspA_{1-186}$, $PspA_{1-110}$, $PspA_{110-222}$, $PspA_{67-186}$, and $PspA_{67-222}$ (Fig. 1). PCR fragments were cloned into pGEMT-easy (Amersham Biosciences) and were inserted into NdeI-HindIII-digested pET28b+ (Novagen). Plasmids pSLEPspA1-186, pSLEPspA1-110, pSLEPspA110-222, pSLEPspA67-222, and pSLEPspA67-186 encode PspA fragments as six-His fusion proteins.

Plasmids encoding full-length PspF or residues 1 to 275 (pSLE40 and pPB1, respectively) were the template for construction of mutant $PspF_{1-275}{}^{W56A}$ using the Quickchange mutagenesis kit (Stratagene). Briefly, mutated DNA was synthesized by *Pfu* DNA polymerase in a reaction containing pSLE40 or pPB1 and a large molar excess of complementary mutagenic oligonucleotides. Following 30 cycles of heating at 95°C for 1 min, 50°C for 1 min, and 68°C for 12 min, the reaction mixtures were treated with DpnI to remove the parental DNA. The resulting reaction was used to transform *E. coli* MC1061 cells. Mutant clones were verified by DNA sequencing. The resulting plasmids, pPB8-W56A and pPB1-W56A, encode $PspF^{W56A}$ and $PspF_{1-275}{}^{W56A}$, respectively, as amino-terminal six-His-tagged fusion proteins.

PspA, PspA fragments, and PspF were amplified by PCR from plasmids pSLE18A, pSLEPspA1-186, pSLEPspA1-110, pSLEPspA110-222, pSLEPspA67-222, pSLEPspA67-186, and pSLE40 using appropriate primers that introduce SacI and KpnI restriction sites and cloned into SacI-KpnI-digested pSR658 and pSR659 vectors (17).

pSLE18A was XbaI-SacI digested, and the *pspA*-containing sequence was cloned into the kanamycin-resistant pAPT110 plasmid (44) so as to express the wild-type PspA protein under the control of a *lacUV5* promoter (pPB9 plasmid). pSLE40 and pSLE40-W56A were XbaI-HindIII digested, and the *pspF*-containing sequences were cloned into the chloramphenicol-resistant pBAD18-Cm (24) so as to express the PspF proteins under the control of the pBAD promoter (pPB8-WT and pPB8-W56A, respectively).

Proteins. *E. coli* core RNA polymerase was purchased from Epicentre technologies. *Klebsiella pneumoniae* σ^{54} protein was purified as described previously

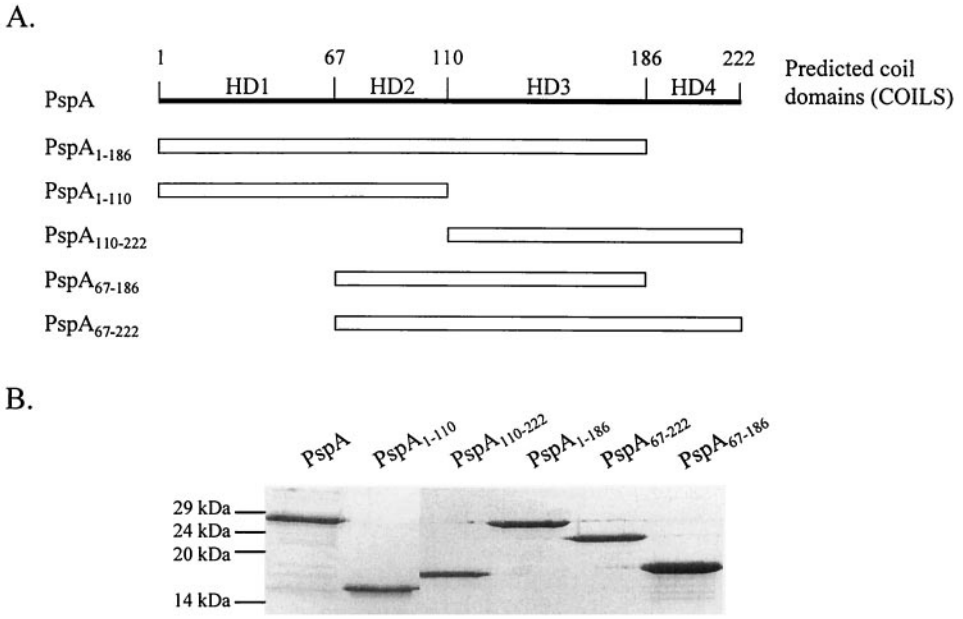

FIG. 1. PspA fragments. (A) Schematic showing (to scale) the predicted four helical domains (HD1 to -4) of *E. coli* PspA using the COILS program. (B) Coomassie blue-stained 18% SDS-PAGE gel showing the PspA fragments purified as six-His fusion proteins.

(9). *E. coli* PspA, $PspF_{1-275}$, and PspF were overproduced and purified as amino-terminal six-His-tagged fusion proteins as described previously (19, 29). PspA fragments were purified as was PspA (19).

Native gel mobility shift assays. A *Sinorhizobium meliloti nifH* (−12/−11) DNA probe for DNA-based assays (σ isomerization) was constructed essentially as described previously (9, 10). Protein binding reactions were conducted in STA buffer (25 mM Tris acetate [pH 8.0], 8 mM Mg acetate, 100 mM KCl, 1 mM dithiothreitol, and 3.5% [wt/vol] PEG-6000) and using 16 nM ^{32}P-end-labeled DNA. σ^{54} was present at 1 μM and dGTP at 4 mM. $PspF_{1-275}$ was preincubated in STA buffer with various amounts (as indicated in the figures) of PspA, PspA fragments, bovine serum albumin (BSA), or PspA storage buffer for 10 min at 30°C prior to addition of the mixture to the σ isomerization assay for 10 min. Protein-DNA complexes were analyzed on a 4.5% native polyacrylamide gel run at 60 V for 80 min in 25 mM Tris, 200 mM glycine buffer (pH 8.6) and were detected by PhosphorImager analysis (Fuji Bas-1500; Tina version 2.10g software).

PspA-PspF binding assays were conducted in STA buffer as described previously (19). Briefly, $PspF_{1-275}$ (5 μM) was incubated with various concentrations of PspA or PspA fragments (as indicated in the figures) for 10 min at 30°C, and protein-protein complexes were analyzed on a 4.5% native polyacrylamide gel run at 4°C. Proteins were visualized by Coomassie staining.

ATP hydrolysis. Assays to measure the ATPase activity of PspF were essentially performed as described previously (19, 46). Briefly, ATPase assays were carried out in reaction buffer (35 mM Tris acetate [pH 8.0], 70 mM K acetate, 5 mM Mg acetate, 19 mM NH_4 acetate, 0.7 mM dithiothreitol). PspF (500 nM) was preincubated with increasing concentrations of PspA or PspA fragments in reaction buffer for 10 min at 30°C. ATPase activity was measured by adding 4 mM ATP containing [α-^{32}P]ATP (0.06 μCi/μl)-ADP. Reactions were stopped after 30 min by adding 5 volumes of 2 M formic acid. Released [α-^{32}P]ADP was separated from [α-^{32}P]ATP using thin-layer chromatography and measured by phosphorimaging.

Bacterial two-hybrid screen and β-galactosidase assays. The PspF and PspA two-hybrid expression plasmids were transformed into the *E. coli* SU101 and SU202 reporter strains to assay homodimerization and heterodimerization, respectively (17). To assay for β-galactosidase activity, overnight cultures in LB with the appropriate antibiotics were diluted 25-fold into the same medium containing 1 mM IPTG (isopropyl-β-D-thiogalactopyranoside). Cultures were incubated at 37°C until the optical density at 600 nm (OD_{600}) reached 0.5. Cells were harvested and assayed for β-galactosidase activities as described by Miller (39). The units were calculated from the results of at least three independent cultures assayed in triplicate.

In vivo inhibition of PspF activity by PspA. *E. coli* strain MVA4 carrying a chromosomal *pspA*::*lacZ* operon fusion was transformed with two compatible plasmids, pPB9 (carrying *pspA* under control of the *lacUV5* promoter) and either pPB8-WT or pPB8-W56A (carrying wild-type *pspF* and mutant *pspFW56A*, respectively, under control of the pBAD promoter). Overnight cultures in LB containing 0.2% glucose and the appropriate antibiotics were diluted 100-fold and grown for 3 h in the same media. Following the addition of 1 mM IPTG and 0.2% arabinose, the cells were grown for 1 h (OD_{600}, ~1.5) and assayed for β-galactosidase activity as described above.

Western blotting. Proteins were separated on a 12.5% sodium dodecyl sulfate (SDS)-polyacrylamide gel and were transferred onto nitrocellulose membranes using a semidry transblot system (Bio-Rad). Anti-LexA (1:4,000 dilution; Invitrogen) and horseradish peroxidase-conjugated anti-mouse immunoglobulin G (1:8,000 dilution; Sigma) antibodies were used for detection with the ECL chemiluminescence system (Pharmacia).

RESULTS

Design, expression, and purification of PspA fragments. The *E. coli pspA* gene encodes the 222-amino-acid PspA protein. PspA is predicted to contain four α-helices that form a coiled-coil structure comprising nearly the entire length of the protein (18). Strikingly, this coiled-coil core is shared by the PspA homologue VIPP1 (1). To elucidate sequences within PspA that are essential for negative regulation of σ^{54}-dependent transcription mediated by PspF, we used a protein fragmentation analysis of PspA. Based on a coiled-coil structure prediction program using the Lupas algorithm (COILS) (36, 37) and multiple sequence alignments (created by the Clustal X program), we identified four putative α-helical domains (HD1 to -4) (Fig. 1A) within the PspA protein. The fragments of PspA were chosen to include a minimum of two predicted α-helical elements (Fig. 1A). The partial sequences of *pspA* were constructed and overproduced as amino-terminal six-His-tagged fusion proteins (Fig. 1B). The fragments are named after the encoding region of PspA that they comprise (i.e., fragment

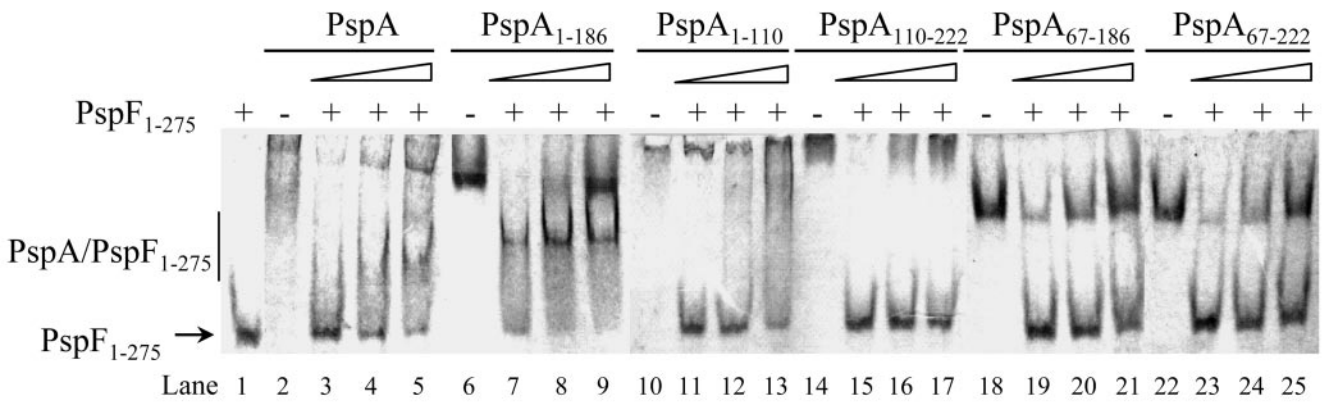

FIG. 2. Interaction between PspA fragments and the AAA domain of PspF ($PspF_{1–275}$). Coomassie-stained native gel showing complex formation between 5 μM $PspF_{1–275}$ and increasing amounts of PspA or PspA fragments (5, 10, and 20 μM). Migration properties of PspA and PspA fragments (20 μM) in the absence (−) of PspF are shown in lanes 2, 6, 10, 14, 18, and 22.

$PspA_{1–186}$ includes residues 1 to 186 of PspA). Fragments $PspA_{1-186}$, $PspA_{1-110}$, $PspA_{67-222}$, and $PspA_{67-186}$ were released from the insoluble cell fraction with CHAPS {3-[(3-cholamidopropyl)-dimethylammonio]-1-propanesulfonate} treatment, as occurs for PspA (19). Fragment $PspA_{110-222}$ was found to be mainly in the soluble fraction. For parity, we chose to include CHAPS in the purification of all PspA fragments (Fig. 1B).

Binding interactions between PspA fragments and the AAA domain of PspF in vitro. We screened for the ability of the five PspA fragments to interact with PspF. In the in vitro assays described hereafter, we used two forms of PspF, either the full-length protein or, for experimental simplicity, a fragment that comprises only the AAA domain ($PspF_{1–275}$) (5). Direct binding of PspA to $PspF_{1–275}$ can be detected using native polyacrylamide gel electrophoresis (PAGE) followed by Coomassie staining and does not require σ^{54} or any other Psp proteins (19). As shown in Fig. 2, no interaction was detected between $PspF_{1–275}$ and PspA fragments $PspA_{110–222}$, $PspA_{67–222}$, and $PspA_{67–186}$. By contrast, $PspA_{1–186}$ and $PspA_{1–110}$ retained the ability to interact with $PspF_{1–275}$, the complex formed by $PspA_{1–110}$ being weaker than those formed by PspA or $PspA_{1–186}$ (Fig. 2, compare lanes 10 to 13 with lanes 3 to 5 and 6 to 9). These results show that the major PspF binding determinants are contained within the three N-terminal α-helical domains of PspA (HD1 to -3) and that the integrity of HD1 is required for complex formation. Notably, the interaction between $PspA_{1–186}$ and $PspF_{1–275}$ leads to a significantly tighter complex, as resolved on native PAGE, than does the interaction between PspA and $PspF_{1–275}$, and this could be partly due to $PspA_{1–186}$ being more homogeneous on native PAGE than PspA (Fig. 2, compare lane 6 to lane 2). Moreover, this tight complex is clearly seen at a 1:1 ratio of $PspF_{1–275}$ to $PspA_{1–186}$, while the complex between $PspF_{1–275}$ and PspA forms at a 1:2 ratio of $PspF_{1–275}$ to PspA. These data suggest that (i) PspA fragment $PspA_{1–186}$ binds $PspF_{1–275}$ with greater affinity and/or in a more stable manner than PspA and (ii) HD4 of PspA destabilizes the complex between PspA and PspF. The latter may be of significance for controlling PspA-PspF interactions and relieving inhibition.

PspA determinants for the inhibition of $PspF_{1–275}$ functionality in vitro. We screened the biochemical activities of the PspA fragments using a number of assays designed to evaluate the contributions of PspA helical domains to the negative control of PspF-dependent open-complex formation. PspA has been shown to inhibit PspF-mediated remodeling (isomerization) of a basal σ^{54}-DNA complex (19). σ^{54}-DNA isomerization by PspF reflects a step in open-complex formation and can be assayed using $PspF_{1–275}$, hydrolyzable nucleotides, and a heteroduplex *S. meliloti* promoter probe that contains a 2-bp mismatch at the −12 and −11 positions (Fig. 3A) [(−12/−11) DNA probe] relative to the transcription start site +1, representing the distorted DNA within the closed complex (9, 41). The efficiency of the activator-driven isomerization of the σ^{54}/(−12/−11) DNA complex can be measured by native PAGE analysis. As shown in Fig. 3A, the isomerized σ^{54}/(−12/−11) DNA complex migrates more slowly, as a supershifted complex [ss σ^{54}/(−12/−11) DNA], on native gels than the nonisomerized initial σ^{54}/(−12/−11) DNA complex (compare lane 3 with lane 2). Preincubation of PspA with $PspF_{1–275}$ leads to 100% inhibition of $PspF_{1–275}$-mediated σ isomerization at a 3:1 ratio of PspA to $PspF_{1–275}$ (Fig. 3A, compare lane 3 with lane 6) (19). Only two PspA fragments, $PspA_{1–186}$ and $PspA_{1–110}$, were found to inhibit $PspF_{1–275}$ remodeling activity (Fig. 3A and data not shown). Complete inhibition of $PspF_{1–275}$-mediated σ isomerization by $PspA_{1–186}$ occurred at a 3:1 ratio of PspA fragment to $PspF_{1–275}$, which was similar to the inhibition caused by PspA (Fig. 3A, compare lanes 7 to 9 with 4 to 6). Inhibition of $PspF_{1–275}$-mediated σ isomerization by $PspA_{1–110}$ was weak, and a much higher concentration of $PspA_{1–110}$ (10:1 ratio of PspA fragment to $PspF_{1–275}$) than PspA or $PspA_{1–186}$ was required to reach ~90% inhibition (Fig. 3A, compare lanes 10 to 14 to lanes 4 to 6 and lanes 7 to 9). We ensured that inhibition by the $PspA_{1–110}$ fragment was specific to the PspA sequences and not due to high protein concentrations per se by preincubating BSA with $PspF_{1–275}$ at a 10:1 ratio. No effect of BSA was detected on the level of $PspF_{1–275}$-mediated σ isomerization (data not shown).

The ATP hydrolysis activity of PspF is required for its ability to activate transcription. The ATPase activity of PspF can be analyzed by using a thin-layer chromatography approach and measuring the release of [α-^{32}P]ADP from radiolabeled [α-^{32}P]ATP under different conditions (46). Previously, we showed that PspA inhibits ATP hydrolysis by PspF (19)

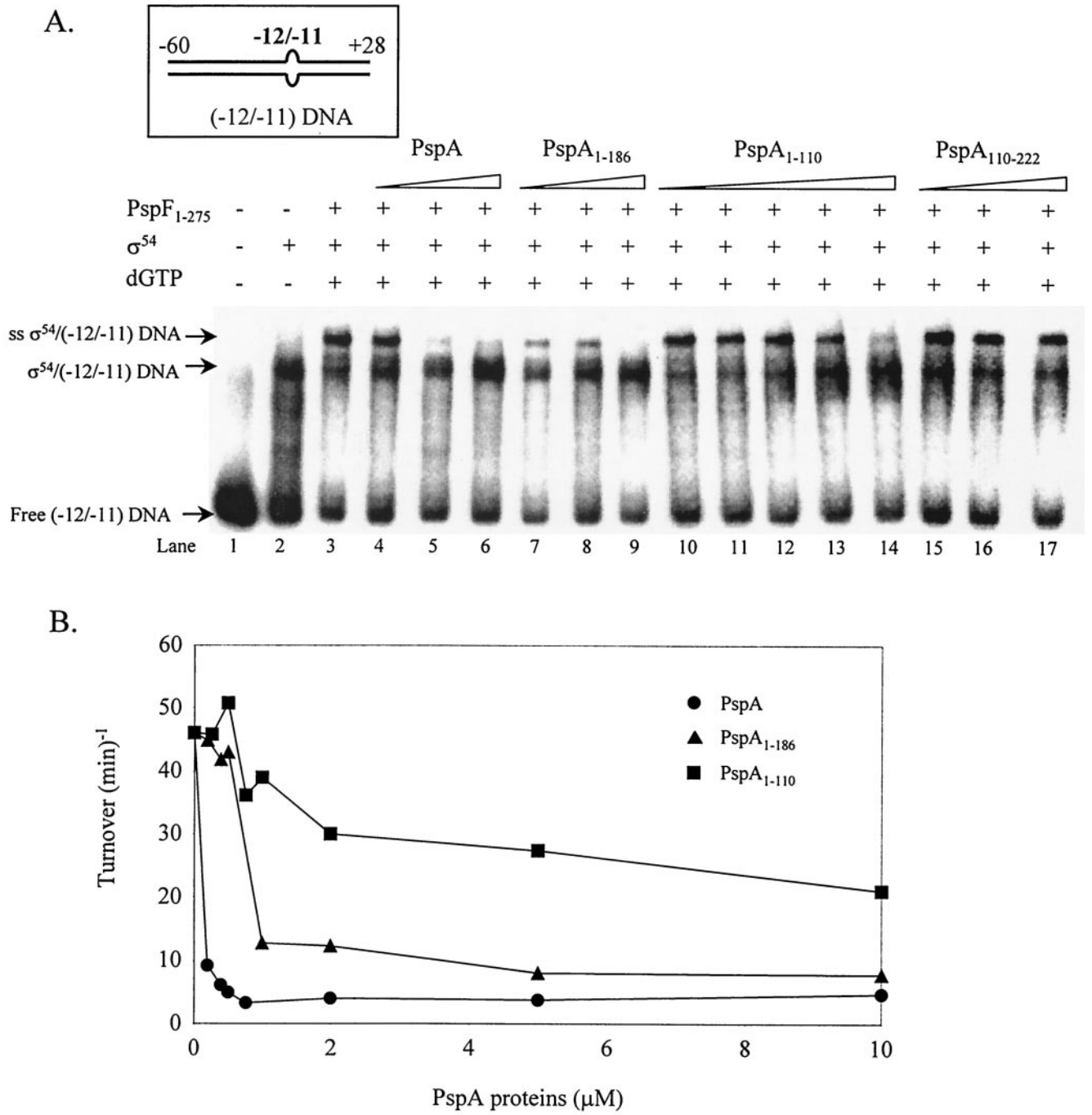

FIG. 3. Effects of PspA fragments on $PspF_{1–275}$ functioning. (A) Native gel showing the effects of PspA fragments on nucleotide-dependent isomerization of σ^{54} bound to (−11/−12) DNA probe by $PspF_{1–275}$ when PspA fragments were preincubated with $PspF_{1–275}$. Reaction mixtures contained (+) 16 nM of ^{32}P-end-labeled *S. meliloti nifH* promoter (−11/−12) DNA probe, 1 μM of σ^{54}, 4 mM dGTP, 1 μM of $PspF_{1–275}$, and increasing concentrations of PspA or PspA fragments (1, 2, and 3 μM for PspA, $Psp_{1–186}$, and $PspA_{110–222}$; 1, 2, 3, 5, and 10 μM for $PspA_{1–110}$). The isomerized complex is marked ss σ^{54}/(−11/−12) DNA. Complexes were detected by PhosphorImager analysis. (B) Effects of PspA fragments on PspF ATPase activity. The ATPase activity of PspF was measured by incubating 500 nM PspF with [α-^{32}P]ATP for 30 min, followed by separation of [α-^{32}P]ATP and [α-^{32}P]ADP on thin-layer chromatography and was quantified by PhosphorImager analysis. The graph shows the amount of ATP turnover of PspF when preincubated with increasing concentrations of PspA or PspA fragments ($PspA_{1–186}$ and $PspA_{1–110}$s) 10 min before the addition of [α-^{32}P]ATP to start the ATP hydrolysis reaction. (C) Native gel showing the effects of the combination of PspA fragments $PspA_{110–222}$ and $PspA_{1–110}$ on nucleotide-dependent isomerization of σ^{54} bound to (−11/−12) DNA probe by $PspF_{1–275}$. σ isomerization reactions were conducted as for panel A. When present (+), PspA was at 3 μM (lane 4). The reactions in lanes 5 to 9 were done using 3 μM $PspA_{1–110}$. In lanes 6 to 8, increasing concentrations of $PspA_{110–222}$ (1, 2, and 3 μM) were added to 3 μM of $PspA_{1–110}$. Lane 9 and lane 15 represent the addition of PspA fragment storage buffer and BSA, respectively, substituted for 3 μM $PspA_{110–222}$. The reactions in lanes 10 to 14 were done using 3 μM $PspA_{110–222}$. In lanes 11 to 13, increasing concentrations of $PspA_{1–110}$ (1, 2, and 3 μM) were added to 3 μM of $PspA_{110–222}$. Lane 14 represents the addition of storage buffer substituted for 3 μM $PspA_{1–110}$.

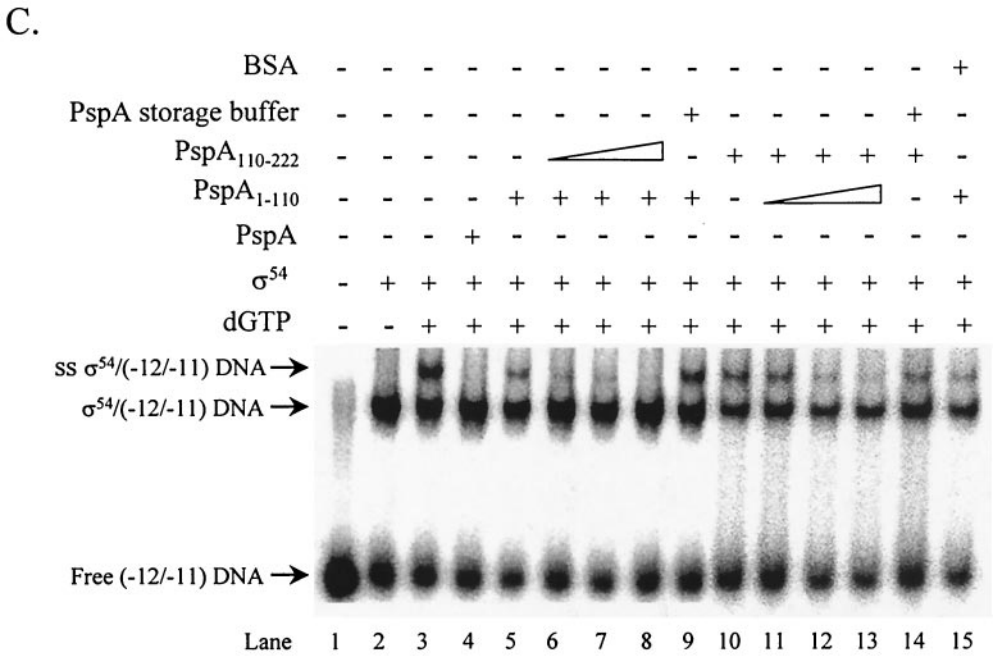

FIG. 3—*Continued*.

(Fig. 3B). $PspA_{1-186}$ and $PspA_{1-110}$ were the only PspA fragments to inhibit PspF-dependent ATP hydrolysis activity (Fig. 3B and data not shown). Compared to the inhibitory effect of PspA, $PspA_{1-186}$ gave a similar marked decline of the ATPase activity of PspF (Fig. 3B), but at a slightly higher concentration of 1 μM compared to 0.2 μM PspA. Interestingly, $PspA_{1-110}$ inhibited PspF ATPase activity, but at 2 μM and less efficiently (Fig. 3B). Overall, these results show that major determinants for the repression of PspF activity are contained within the three N-terminal α-helical domains of PspA (HD1 to -3). Thus, there is a strong correlation between the abilities of PspA to repress PspF functionality and to bind directly to PspF, implying that the determinants for these dominant physical interactions between PspA and PspF are required for the inhibitory effect of PspA.

We then addressed the issue of whether the C-terminal region of PspA ($PspA_{110-222}$; HD3 to -4) could stimulate the weak activity of the N-terminal region of PspA ($PspA_{1-110}$; HD1 to -2) as though it were within the full-length PspA protein. We preincubated $PspA_{1-110}$ with increasing concentrations of $PspA_{110-222}$ and assayed the inhibitory effect of the mixture on $PspF_{1-275}$-mediated σ isomerization. The results showed that the addition of $PspA_{110-222}$ to $PspA_{1-110}$ increases the inhibitory activity of $PspA_{1-110}$ to levels similar to those of the inhibition caused by PspA (Fig. 3C, compare lane 8 to lane 4). The reciprocal experiment, in which increasing concentrations of $PspA_{1-110}$ were preincubated with $PspA_{110-222}$, also resulted in clear repression of $PspF_{1-275}$ activity, consistent with the former experiment (Fig. 3C, lanes 6 to 8). Control experiments were performed to ensure that none of the concentrations of $PspA_{110-222}$ used in this assay had any inhibitory effect on $PspF_{1-275}$-mediated σ isomerization (Fig. 3A and data not shown) and that the activity was specific to PspA sequences, since replacing one of the PspA fragments with BSA or with PspA storage buffer did not stimulate the inhibitory activity of the other PspA fragment (Fig. 3C and data not shown). A similar recovery of the activity of $PspA_{1-110}$ by adding increasing concentrations of $PspA_{110-222}$ was observed when we tested the inhibition of PspF-dependent ATP hydrolysis (data not shown). These results suggest that there are determinants in the C-terminal domains HD3 and HD4 that are required for the functioning of PspA as a negative regulator of PspF and that interactions between the N-terminal and C-terminal helical domains are required for the full inhibition of PspF activity in vitro, possibly by stabilizing the interaction of PspF with the N-terminal part of PspA or through formation of a higher-order structure of PspA.

Binding interactions between PspA fragments and the AAA domain of PspF in vivo. We showed previously that PspA and PspF interact in vitro (19). To determine whether PspA and the PspA fragments could interact with PspF in vivo and therefore to establish that our in vitro binding assays reflected faithfully the in vivo situation, we took advantage of a LexA-based genetic system for studying protein-protein interactions in an *E. coli* background (13, 17). The bacterial transcriptional repressor LexA has two domains, an N-terminal DBD and a C-terminal dimerization domain. A truncated LexA consisting of only the DBD can recognize its operator sequence, but it is functional as a transcriptional repressor only in a dimeric form. Other proteins can be fused in frame to the DBD and will restore the repressor's function if these domains interact. Since PspA and PspF can both form higher-order oligomers (12, 25), we used a modified system that is sensitive only to the formation of heterodimers (17). The PspA and PspF proteins were, respectively, fused to a wild-type (plasmid pRS658) and a mutant (plasmid pRS659) LexA DBD. Their heteroassociation was specifically measured by the transcriptional repression of the reporter gene *lacZ*, controlled by a hybrid operator, *sulA*,

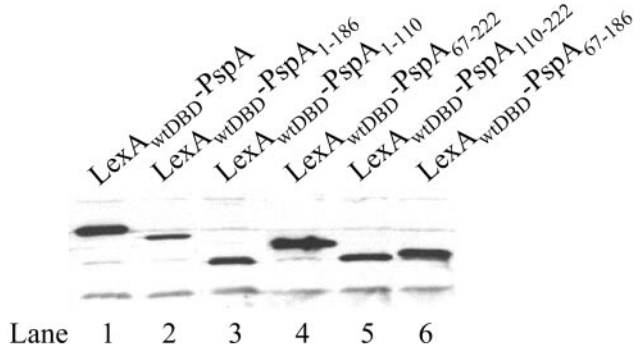

FIG. 4. Western blot analysis of LexA$_{wtDBD}$-PspA fragment fusion proteins. LexA$_{wtDBD}$-PspA fragment fusions were expressed in *E. coli* SU202 using 1 mM IPTG. An immunoblot of crude lysates of IPTG-induced cultures (OD_{600}, ~0.5) probed with anti-LexA antiserum (Invitrogen) is shown. The calculated molecular masses (in kilodaltons) for the LexA fusions are in parentheses: lane 1, LexA-PspA (34.6); lane 2, LexA-PspA$_{1–186}$ (30.4); lane 3, LexA-PspA$_{1–110}$ (21.5); lane 4, LexA-PspA$_{1–67}$ (16.5); lane 5, LexA-PspA$_{67–222}$ (27); lane 6, LexA-PspA$_{110–222}$ (22); lane 7, LexA-PspA$_{67–186}$ (22.9).

containing a wild-type half-site and a mutated operator half-site. The identities and production of the LexA fusion proteins were verified by Western blot analysis using an antibody raised to the LexA protein (Fig. 4 and data not shown). Only those fusion proteins that repressed expression of β-galactosidase at a reproducible level of ≥25% of the controls were considered to be interacting efficiently (13). As shown in Table 2, we observed a significant interaction between PspA and PspF, quantitated as 69% repression of β-galactosidase activity in cells harboring the LexA-PspA fusion expressed from the pSR658 vector and the LexA-PspF fusion in the pSR659 vector and as 73% repression of β-galactosidase activity in the reciprocal experiment. The heterodimerization between PspA and PspF was slightly less efficient than the multimerization of PspA or PspF when the proteins were expressed from pSR658 and tested with a wild-type LexA-based genetic system PspA, with 83% and 84% repression of β-galactosidase activity, respectively (data not shown). Further, the results showed that only the PspA fragment PspA$_{1–186}$ was able to significantly interact with PspF (Table 2). The interaction results were evident and reproducible in the reciprocal experiment with opposite vector pairs (data not shown). Although PspA$_{1–110}$ interacts with PspF$_{1–275}$ in vitro, no evidence for a complex was detected between PspA$_{1–110}$ and PspF in vivo (Table 2), possibly suggesting that other determinants are required for stable complex formation between PspA$_{1–110}$ and PspF in vivo.

TABLE 2. Interactions between PspA fragments and PspF using an in vivo bacterial two-hybrid system in *E. coli*

Fusion[a]		% repression[b] (mean ± SD)
pRS658	pSR659	
pspA	*pspF*	69 ± 1
pspF	*pspA*	73 ± 1
pspA$_{1-186}$	*pspF*	65 ± 6
pspA$_{1-110}$	*pspF*	26 ± 3
pspA$_{110-222}$	*pspF*	0 ± 6
pspA$_{67-222}$	*pspF*	19 ± 9
pspA$_{67-186}$	*pspF*	2 ± 5
pspA	*pspFW56A*	38 ± 0.8

[a] Gene fused to either the wild-type *lexA* DBD (pSR658) or the mutant *lexA* DBD (pSR659).

[b] Percent repression of β-galactosidase activity relative to strain SU202 with pSR658 and pSR659 alone. The average activity of the vector control was 4,689 ± 246 Miller units (nonrepressed activity).

We tested whether the PspA fragments with established in vitro activities were able to inhibit PspF function in vivo by using primer extension to assess the levels of *pspA* transcription from cells overexpressing either the LexA-PspA fusion, the LexA-PspA fragment fusions, or the DBD of LexA on its own as a control (data not shown). Only PspA$_{1–186}$ inhibited transcription of *pspA* to a level similar to that of PspA (data not shown), fully consistent with repression data from the bacterial two-hybrid system. Overall, these results indicate that HD4 of PspA is dispensable for the interaction of PspA with PspF and for the inhibition of PspF-dependent activation of transcription in vivo and in vitro.

Identification of a putative PspF binding site for PspA. Previous characterization of PspA function suggested that PspA prevented or altered the self-association of PspF, which in turn inhibited PspF ATPase activity (18, 19, 25). Given that the major determinants for self-association and ATPase activity are contained within the AAA domain of PspF, we postulated that PspA could bind to surface-exposed regions of the AAA domain of PspF and that these regions should be located close to the protomer-protomer interface and the ATPase active site. In addition, since PspA inhibits specifically the activity of PspF and not other AAA activators of the σ^{54}-RNAP (19), PspA-interacting surfaces on PspF may well be unique to PspF. To identify these specialized regions, we used a bioinformatics-based approach. We created a sequence alignment of PspF proteins from different bacterial species (*Yersinia pestis*, *Yersinia enterocolitica*, *Salmonella enterica* serovar Typhimurium, *E. coli*, *Vibrio cholerae*, and *Klebsiella pneumoniae*) using the Clustal X and Genedoc programs to identify conserved amino acids within PspF (data not shown). This was amalgamated with a sequence alignment of the σ^{54} AAA activators NifA and NtrC from different species to identify conserved residues specific to PspF (data not shown). Once identified, these residues were then mapped onto a theoretical model of the hexameric ring of the AAA domain of PspF (PspF$_{1–275}$) derived from the crystal structure of the AAA activator NtrC1 from *Aquifex aeolicus* (Fig. 5) (34). The single amino acid that matched the criteria we imposed is W56 (Fig. 5).

To probe the function of W56 in PspF$_{1–275}$, we used a site-directed mutagenesis approach to replace the tryptophan residue with alanine, the residue found in most NtrC and NifA homologues. PspF$_{1–275}^{W56A}$ was purified as an N-terminal histidine-tagged fusion protein and was soluble and homogeneous as judged by SDS-PAGE analysis (data not shown). The mutant PspF$_{1–275}$ protein was tested using a range of in vitro assays reflecting different steps of the activation pathway and compared to wild-type PspF$_{1–275}$ activity. These included (i) ATP hydrolysis activity (46); (ii) stable oligomer formation in the presence of ADP · AlF_x, a transition state analogue of ATP at the point of hydrolysis (12); (iii) ADP · AlF_x-dependent binding to σ^{54} (12); (iv) σ isomerization (9); and (v) activation of the σ^{54}-RNAP (5). The results showed that PspF$_{1–275}^{W56A}$ had wild-type-like functioning in vitro (data not shown). Thus,

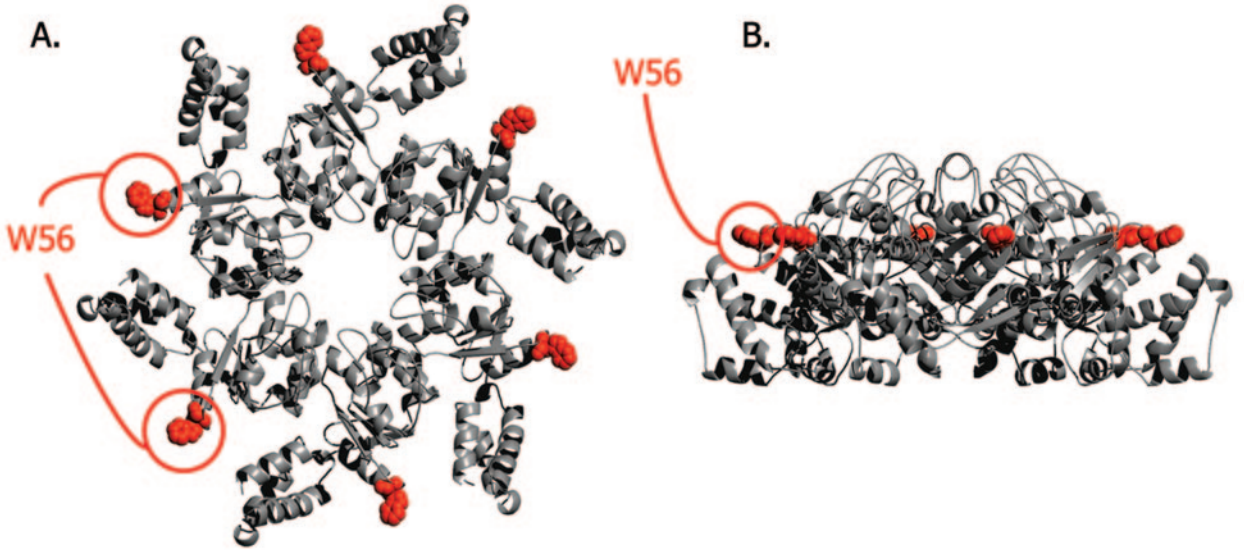

FIG. 5. Theoretical atomic model of a $PspF_{1–275}$ hexamer highlighting the probable location of W56. The model was prepared by submitting the sequence of the PspF AAA domain to the 3D-JIGSAW comparative-modeling server (http://www.bmm.icnet.uk/servers/3djigsaw/). The server builds three-dimensional models for proteins based on homologues of known structures (2). Theoretical coordinates for residues P31 to V237 were obtained based on the crystal structure of NtrC1 (34) (Protein Data Base [PDB] entry, 1NY5) with 95% accuracy. The high accuracy of the model is linked to the high sequence identity between PspF and NtrC1 sequences for the region of interest: 50.5%. Because the AAA domain of p97 crystallized as a hexamer, the model was superimposed onto the D1 structure of p97, including residues 200 to 458 (52) (PDB entry, 1E32), using the computer program CCP4-GUI. An accurate superposition was obtained due to the high secondary-structure conservation among AAA domains. A theoretical PspF hexamer was then generated using the CCP4-GUI. The figures were prepared using Pymol (http://pymol.sourceforge.net/) and POV-Ray (http://www.povray.org/). (A) Top view of a theoretical $PspF_{1-275}$ hexamer shown in a grey cartoon representation. W56 in individual monomers is shown in a red-sphere representation. The probable locations of two of the six W56s are further highlighted using red circles. (B) Side view of the same hexamer with the putative location of one W56 highlighted using a red circle.

the single-amino-acid substitution W56A had no detrimental effects on the properties of $PspF_{1–275}$ required for transcription activation of the σ^{54}-RNAP.

The $PspF_{1–275}^{W56A}$ mutant is insensitive to PspA negative regulation in vitro. If the W56 residue of PspF is a target for PspA binding, then $PspF_{1–275}^{W56A}$ should be less sensitive to PspA-dependent inhibition. To address this issue, we examined the effect of PspA on $PspF_{1–275}^{W56A}$-dependent isomerization of the σ^{54}/(−12/−11) DNA complex. In the absence of PspA, wild-type PspF and $PspF_{1–275}^{W56A}$ show similar levels of σ isomerization (Fig. 6A, compare lane 3 to lane 6). In contrast to wild-type PspF, the preincubation of increasing concentrations of PspA with $PspF_{1–275}^{W56A}$ resulted in no significant inhibition of σ isomerization (Fig. 6A, compare lanes 3 to 5 with lanes 6 to 8). These results suggest that $PspF_{1–275}^{W56A}$ is insensitive to PspA inhibitory function in vitro.

To determine whether this loss of sensitivity to PspA inhibition could be due to a lack of interaction with PspA, we tested whether $PspF_{1–275}^{W56A}$ could bind PspA in vitro. Increasing concentrations of PspA were incubated with either wild-type $PspF_{1–275}$ or $PspF_{1–275}^{W56A}$, and the reaction products were analyzed by native PAGE and Coomassie staining (Fig. 6B). $PspF_{1–275}^{W56A}$ migrates slightly faster than wild-type $PspF_{1–275}$ on a native gel, probably because of the loss of the hydrophobic side chain of the tryptophan residue. Mutant $PspF_{1–275}^{W56A}$ did not detectably bind PspA compared to wild-type $PspF_{1–275}$ (Fig. 6B, compare lanes 6 to 9 with lanes 2 to 5). These data suggest that the inability of PspA to inhibit $PspF_{1–275}^{W56A}$ is due to the inability of PspA to form an inhibitory complex with $PspF_{1–275}^{W56A}$.

PspA is not able to act as a negative regulator of the $PspF^{W56A}$ mutant in vivo. Using the same LexA-based bacterial two-hydrid system described above, we measured heteroassociation between PspA and $PspF^{W56A}$. As shown in Table 2 and in agreement with our in vitro binding assay, we observed only a weak interaction between PspA and $PspF^{W56A}$, quantitated as 38% repression of β-galactosidase activity in cells harboring the LexA-PspA fusion expressed from the pSR658 vector and the LexA-PspF fusion in the pSR659 vector. These data indicate that W56 of PspF is a major binding determinant for PspA, and the residual repression of β-galactosidase activity suggests that interactions between PspA and PspF independent of W56 do occur in vivo.

To examine whether the W56A substitution in PspF could alter the inhibitory effect of PspA on PspF-dependent activation of transcription in vivo, we developed an in vivo assay. *E. coli* MVA4 is a derivative of MC1061 and carries a *pspA*::*lacZ* chromosomal fusion (Ap^r). MVA4 was transformed with two compatible plasmids (Fig. 7): pPB9 (Km^r), carrying *pspA* under control of the *lacUV5* promoter, and either pPB8-WT or pPB8-W56A (Cm^r), carrying wild-type *pspF* and mutant *pspFW56A*, respectively, under control of the pBAD promoter. As expected, the overexpression of the wild-type PspF by adding 0.2% arabinose to the cultures resulted in the activation of the chromosomal *pspA*::*lacZ* (fourfold increase) (Fig. 7A). The simultaneous induction of PspA expression with 1 mM IPTG

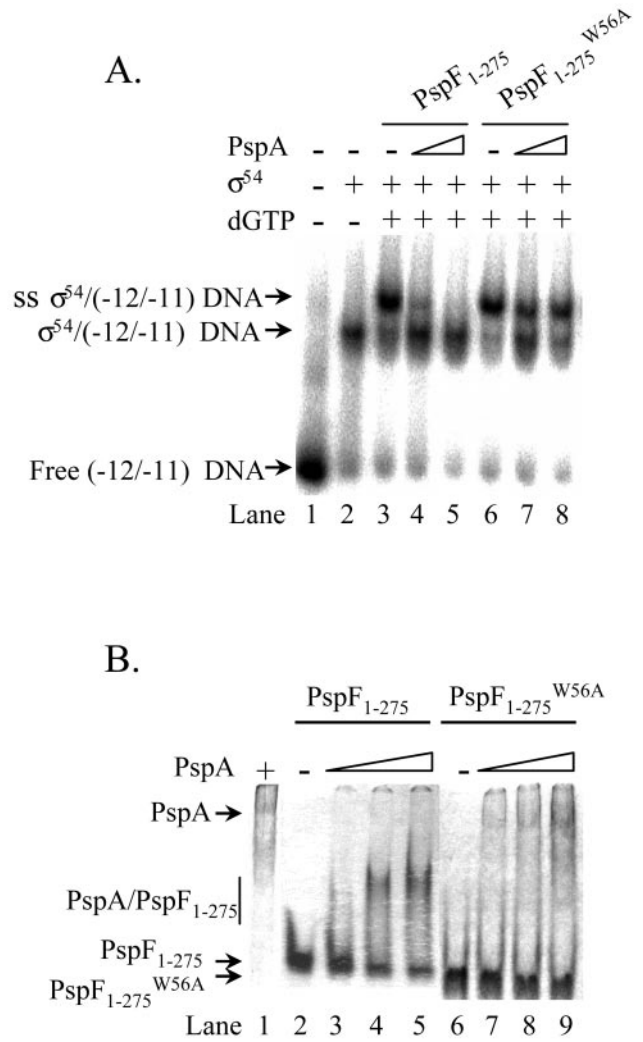

FIG. 6. $PspF_{1–275}^{W56A}$ escapes the inhibitory actions of PspA in vitro. (A) Native gel showing the effects of PspA on nucleotide-dependent isomerization of σ^{54} bound to (−11/−12) DNA probe by either $PspF_{1–275}$ or $PspF_{1–275}^{W56A}$ (1 μM) when increasing PspA fragments (2 and 3 μM) were preincubated with $PspF_{1–275}$ proteins. Reactions were as in Fig. 3, and complexes were detected by PhosphorImager analysis. (B) Coomassie-stained native gel showing complex formation between PspA and either wild-type $PspF_{1–275}$ or mutant $PspF_{1–275}^{W56A}$. Binding reactions were conducted with 5 μM $PspF_{1–275}$ (lanes 2 to 5) or $PspF_{1–275}^{W56A}$ (lanes 6 to 9) with increasing concentrations of PspA (0, 5, 10, and 15 μM).

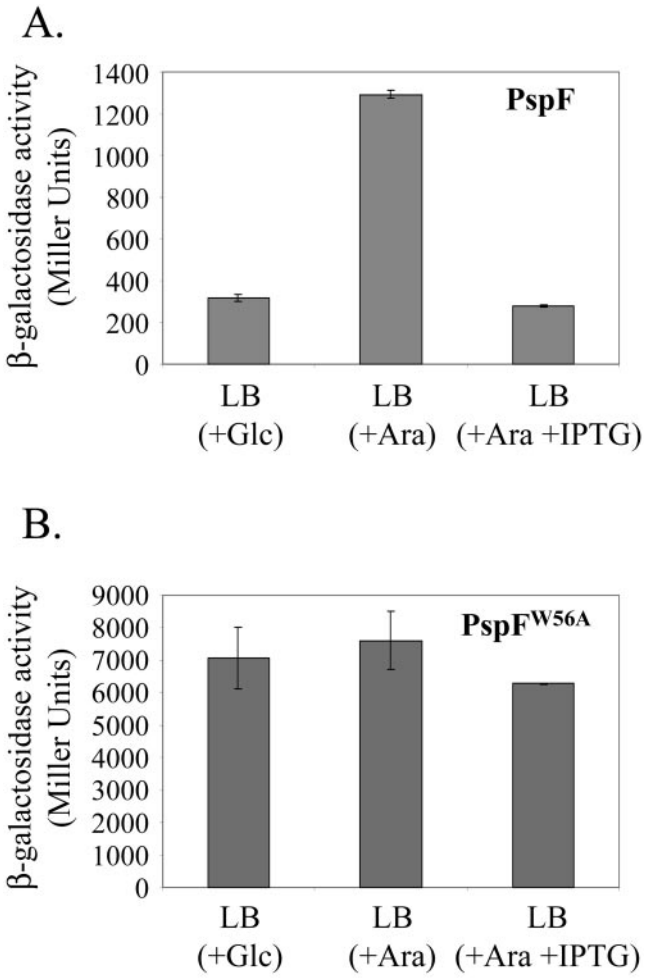

FIG. 7. In vivo effect of PspA on $PspF_{1–275}^{W56A}$-dependent activation of the *pspA* promoter. *E. coli* strain MVA4 carrying a chromosomal fusion, *pspA*::*lacZ*, was transformed with compatible plasmids pPB9, carrying *pspA* under control of placUV5, and either pPB8-WT (A) or pPB8-W56A (B), carrying wild-type *pspF* and mutant *pspFW56A*, respectively, under control of pBAD. Overnight cultures were diluted 100-fold, and cultures were grown at 37°C in LB medium supplemented with 0.2% glucose (to minimize the leaky expression from the placUV5 and pBAD promoters). After 3 h, overexpression of PspA and PspF proteins were induced by adding 1 mM IPTG and 0.2% arabinose for 1 h, and β-galactosidase activities were determined as described in Materials and Methods. The error bars indicate standard deviations.

dramatically decreased β-galactosidase activity to background levels (i.e., in the absence of overproduced PspF). Control experiments in which we used the template plasmids without the *psp* gene showed no effect on the levels of β-galactosidase expression (data not shown). These results are fully consistent with PspA being a negative regulator of PspF and validate the use of this in vivo assay to determine the action of PspA upon PspF. We repeated the assay with the $PspF^{W56A}$ mutant protein (Fig. 7B). Strikingly, overproduced $PspF^{W56A}$ showed a higher β-galactosidase activity than overproduced PspF, since we observed an ~6-fold increase (compare Fig. 7B to A). In addition, in the absence of IPTG, the β-galactosidase activities measured with and without inducing the overexpression of $PspF^{W56A}$ were not significantly different (Fig. 7B). These data suggest that the leaky expression of $PspF^{W56A}$ can stimulate the transcription of the chromosomal wild-type *pspA* promoter, possibly because chromosomally encoded PspA can no longer inhibit the functioning of the $PspF^{W56A}$ mutant. In agreement with this hypothesis, the IPTG-dependent overexpression of PspA did not decrease the activity of $PspF^{W56A}$ as measured by the levels of β-galactosidase activity (Fig. 7B). The use of the same assay based on $PspF_{1–275}$ derivatives confirmed these results (data not shown). The results clearly demonstrate the physiological relevance of the $PspF^{W56A}$ mu-

tation, since they indicate that PspA cannot act effectively as a negative regulator of the $PspF^{W56A}$ mutant in vivo.

DISCUSSION

PspA is the specific negative regulator of the transcriptional activator PspF of the *psp* operon of *E. coli*, a representative of the AAA activators of the σ^{54}-RNAP. The experiments described here were designed to identify the molecular determinants of the inhibitory interaction between PspA and PspF. This analysis depended to a large extent on the availability (i) of biochemically active partial PspA sequences, which had not previously been described, and (ii) of structural data on AAA activators of the σ^{54}-RNAP.

PspA helical domains involved in PspF inhibition. Protein structure prediction programs allowed us to divide the PspA protein into four α-helical domains, reflecting one probable structural organization of PspA. Our results showed that only two PspA fragments were biochemically active in vitro, $PspA_{1–186}$ and $PspA_{1–110}$. $PspA_{1–186}$ was as active as PspA for PspF binding and inhibition, demonstrating that the major PspF inhibitory determinants are contained within the three N-terminal α-helical domains of PspA. Interestingly, $PspA_{1–186}$ seems to bind $PspF_{1–275}$ with a greater affinity than PspA. Nevertheless, $PspA_{1–186}$ displays a similar but not a higher activity than PspA in functional assays for inhition of PspF (i.e., the inhibition of the ATPase activity of PspF). We propose that differences seen in native PAGE assays arise from different conformations of PspF being differently sensitive to PspA, since the gel shift assay is a nonequilibrium binding assay, whereas the functional inhibition assays are equilibrium assays in which PspF can adopt a range of conformations during its ATPase cycle. The activity of $PspA_{1–110}$ was weaker than that of PspA or $PspA_{1–186}$ and could be stimulated by the addition in *trans* of $PspA_{110–222}$. These data suggest that (i) the C-terminal part of PspA contains PspF inhibitory sequences (notably in the HD3) and/or some stabilizing elements for PspA-PspF complex formation and (ii) the N- and C-terminal parts of PspA can partially function as independent domains.

The use of a bacterial two-hybrid system confirmed our in vitro results and provided clear evidence for direct protein-protein interaction between PspA and PspF in vivo in *E. coli*. In addition, the strict correlations between the inhibitory activity of PspA or PspA fragments on PspF and complex formation between PspA or PspA fragments and PspF strongly suggest that PspA-mediated inhibition of PspF must occur through direct protein-protein interactions.

PspA is closely related to Vipp1, which is essential for the formation of the thylakoid membrane in cyanobacteria and chloroplasts. The α-helical domains of Vipp1 and PspA adopt very similar high-molecular-mass oligomeric structures (1, 25). It has been demonstrated for Vipp1 that oligomer formation is important for proper positioning at the inner envelope of chloroplasts and that it involves the interaction of the central α-helical domain common to PspA. Three-dimensional reconstruction data demonstrated that PspA also formed a higher-order oligomeric ring of 36 PspA molecules (25). Although the exact significance of higher-order oligomer formation is not known for PspA, it may be significant for binding and inhibiting PspF, either by preventing nucleotide access to the active site or by inhibiting formation of the correct oligomeric form (19, 25). Together, our findings suggest that the α-helical domains HD1 to -3 of PspA are required for multimerization of PspA and that the C-terminal region of PspA could help in stabilizing higher-order oligomer formation of PspA.

W56 residue of PspF. Since the $PspF^{W56A}$ mutant could not form a detectable complex with PspA and escaped PspA-mediated inhibition in vitro and in vivo, we propose that W56 of PspF is a binding determinant for PspA. Interestingly, W56 appears to lie at the periphery of the modeled $PspF_{1–275}$ hexamer in the α/β subdomain of the AAA core (Fig. 5). More striking is the fact that it is solvent exposed, thus making it directly available for any potential hydrophobic interaction. In agreement with W56 being a major determinant for PspA interaction, compilation and analysis of a database of alanine mutants of heterodimeric protein-protein complexes showed that tryptophan, arginine, and tyrosine residues are preferred in the high-energy interactions between proteins in a heterodimer (4).

We investigated the possibility that the in *trans* PspA-mediated inhibition of PspF could be related to the negative regulation of the activities of other more conventional σ^{54} AAA activators by their in *cis* regulatory domains. We chose to compare PspF with *A. aeolicus* NtrC1, since the receiver domain of NtrC1 negatively controls the activity of its AAA domain and the crystal structures of the AAA domain and the adjacent receiver domain of NtrC1 have been determined (34). In principle, PspA could use a binding surface on PspF equivalent to that used by the receiver domain of NtrC1 to inhibit the functioning of the AAA domain of NtrC1. Although the residue equivalent to W56 in NtrC1 is not coincident to the surface that interacts with the receiver domain, the adjacent residue equivalent to R55 in NtrC1 is very close to where the receiver domain directly interacts, suggesting that the receiver domains of σ^{54} AAA activators, such as NtrC1 and PspA, might use adjacent or possibly slightly overlapping surfaces. However, the mechanism of inhibition may well be different.

ACKNOWLEDGMENTS

This work was supported by a Wellcome Trust project grant. S.E. was the recipient of a BBSRC postgraduate award. P.B. was supported by a BBSRC project grant.

We thank Goran Jovanovic, Antony Mayhew, and Louise Lloyd for useful comments on the manuscript. We thank Xiaodong Zhang for help with the mapping of W56 onto the PspF structural model. We thank D. Daines for the gift of the bacterial two-hybrid system, M. P. Castanié-Cornet for the gift of pAPT110, and J. Beckwith for the gift of pBAD18-Cm.

REFERENCES

1. **Aseeva, E., F. Ossenbuhl, L. A. Eichacker, G. Wanner, J. Soll, and U. C. Vothknecht.** 2004. Complex formation of Vipp1 depends on its alpha-helical PspA-like domain. J. Biol. Chem. **279:**35535–35541.
2. **Bates, P. A., L. A. Kelley, R. M. MacCallum, and M. J. E. Sternberg.** 2001. Enhancement of protein modelling by human intervention in applying the automatic programs 3D-JIGSAW and 3D-PSSM. Proteins **5**(Suppl.)**:**39–46.
3. **Beloin, C., J. Valle, P. Latour-Lambert, P. Faure, M. Kzreminski, D. Balestrino, J. A. Haagensen, S. Molin, G. Prensier, B. Arbeille, and J.-M. Ghigo.** 2004. Global impact of mature biofilm lifestyle on *Escherichia coli* K-12 gene expression. Mol. Microbiol. **51:**659–674.
4. **Bogan, A. A., and K. S. Thorn.** 1998. Anatomy of hot spots in protein interfaces. J. Mol. Biol. **280:**1–9.
5. **Bordes, P., S. R. Wigneshweraraj, J. Schumacher, X. Zhang, M. Chaney, and M. Buck.** 2003. The ATP hydrolyzing transcription activator phage shock protein F of *Escherichia coli*: identifying a surface that binds σ^{54}. Proc. Natl. Acad. Sci. USA **100:**2278–2283.

6. **Brissette, J. L., M. Russel, L. Weiner, and P. Model.** 1990. Phage shock protein, a stress protein of *Escherichia coli*. Proc. Natl. Acad. Sci. USA **87:**862–866.
7. **Brissette, J. L., M. Russel, L. Wiener, and P. Model.** 1991. Characterisation and sequence of the *Escherichia coli* stress induced *psp* operon. J. Mol. Biol. **220:**35–48.
8. **Buck, M., M. T. Gallegos, D. J. Studholme, Y. Guo, and J. D. Gralla.** 2000. The bacterial enhancer-dependent σ^{54} (σ^{N}) transcription factor. J. Bacteriol. **182:**4129–4136.
9. **Cannon, W., M. T. Gallegos, and M. Buck.** 2000. Isomerisation of a binary sigma-promoter DNA complex by transcription activators. Nat. Struct. Biol. **7:**594–600.
10. **Cannon, W., M. T. Gallegos, P. Casaz, and M. Buck.** 1999. Amino-terminal sequences of σ^{N} (σ^{54}) inhibit RNA polymerase isomerization. Genes Dev. **13:**357–370.
11. **Casadaban, M. J., and S. N. Cohen.** 1980. Analysis of gene control signals by DNA fusion and cloning in *Escherichia coli*. J. Mol. Biol. **138:**179–207.
12. **Chaney, M., R. Grande, S. R. Wigneshweraraj, W. Cannon, P. Casaz, M. T. Gallegos, J. Schumacher, S. Jones, S. Elderkin, A. E. Dago, E. Morett, and M. Buck.** 2001. Binding of transcriptional activators to σ^{54} in the presence of the transition state analog ADP-aluminumfluoride: insights into activator mechanochemical action. Genes Dev. **15:**2282–2294.
13. **Daines, D. A., and R. P. Silver.** 2000. Evidence for multimerization of Neu proteins involved in polysialic acid synthesis in *Escherichia coli* K1 using improved LexA-based vectors. J. Bacteriol. **182:**5267–5270.
14. **Darwin, A., and V. Miller.** 2001. The *psp* locus of *Yersinia enterocolitica* is required for virulence and for growth *in vitro* when the Ysc type III secretion system is produced. Mol. Microbiol. **39:**429–444.
15. **Darwin, A., and V. Miller.** 1999. Identification of *Yersinia enterocolitica* genes affecting survival in an animal host using signature-tagged transposon mutagenesis. Mol. Microbiol. **32:**51–62.
16. **DeLisa, M. P., P. Lee, T. Palmer, and G. Georgiou.** 2004. Phage shock protein PspA of *Escherichia coli* relieves saturation of protein export via the Tat pathway. J. Bacteriol. **186:**366–373.
17. **Dmitrova, M., G. Younes-Cauet, P. Oertel-Buchheit, D. Porte, M. Schnarr, and M. Granger-Schnarr.** 1998. A new LexA-based genetic system for monitoring and analyzing protein heterodimerization in *Escherichia coli*. Mol. Gen. Genet. **257:**205–212.
18. **Dworkin, J., G. Jovanovic, and P. Model.** 2000. The PspA protein of *Escherichia coli* is a negative regulator of σ^{54}-dependent transcription. J. Bacteriol. **182:**311–319.
19. **Elderkin, S., S. Jones, J. Schumacher, D. Studholme, and M. Buck.** 2002. Mechanism of action of the *Escherichia coli* phage shock protein PspA in repression of the AAA family transcription factor PspF. J. Mol. Biol. **320:**23–37.
20. **Eriksson, S., S. Lucchini, A. Thompson, M. Rhen, and J. C. Hinton.** 2003. Unravelling the biology of macrophage infection by gene expression profiling of intracellular *Salmonella enterica*. Mol. Microbiol. **47:**103–118.
21. **Gabel, C. V., and H. C. Berg.** 2003. The speed of the flagellar rotary motor of *Escherichia coli* varies linearly with proton motive force. Proc. Natl. Acad. Sci. USA **100:**8748–8751.
22. **Green, R. C., and A. J. Darwin.** 2004. PspG, a new member of the *Yersinia enterocolitica* phage shock protein regulon. J. Bacteriol. **186:**4910–4920.
23. **Guo, Y., C. M. Lew, and J. D. Gralla.** 2000. Promoter opening by σ^{54} and σ^{70} RNA polymerases: σ factor-directed alterations in the mechanism and tightness of control. Genes Dev. **14:**2242–2255.
24. **Guzman, L. M., D. Belin, M. J. Carson, and J. Beckwith.** 1995. Tight regulation, modulation, and high-level expression by vectors containing the arabinose PBAD promoter. J. Bacteriol. **177:**4121–4130.
25. **Hankamer, B. D., S. L. Elderkin, M. Buck, and J. Nield.** 2004. Organization of the AAA^{+} adaptor protein PspA is an oligomeric ring. J. Biol. Chem. **279:**8862–8866.
26. **Ize, B., I. Porcelli, S. Lucchini, J. C. Hinton, B. C. Berks, and T. Palmer.** 2004. Novel phenotypes of *Escherichia coli tat* mutants revealed by global gene expression and phenotypic analysis. J. Biol. Chem. **279:**47543–47554.
27. **Jones, S. E., L. J. Lloyd, K. K. Tan, and M. Buck.** 2003. Secretion defects that activate the phage shock response of *Escherichia coli*. J. Bacteriol. **185:**6707–6711.
28. **Jovanovic, G., L. Weiner, and P. Model.** 1996. Identification, nucleotide sequence, and characterization of PspF, the transcriptional activator of the *Escherichia coli* stress-induced *psp* operon. J. Bacteriol. **178:**1936–1945.
29. **Jovanovic, G., J. Rakonjac, and P. Model.** 1999. *In vivo* and *in vitro* activities of the *Escherichia coli* sigma54 transcription activator, PspF, and its DNA-binding mutant, PspFΔHTH. J. Mol. Biol. **285:**469–483.
30. **Kleerebezem, M., and J. Tommassen.** 1993. Expression of the *pspA* gene stimulates efficient protein export in *Escherichia coli*. Mol. Microbiol. **7:**947–956.
31. **Kleerebezem, M., W. Crielaard, and J. Tommassen.** 1996. Involvement of the stress protein PspA (Phage shock protein A) of *Escherichia coli* in maintenance of the proton motive force under stress conditions. EMBO J. **15:**162–171.
32. **Kroll, D., K. Meierhoff, N. Bechtold, M. Kinoshita, S. Westphal, U. C. Vothknecht, J. Soll, and P. Westhoff.** 2001. VIPP1, a nuclear gene of *Arabidopsis thaliana* essential for thylakoid membrane formation. Proc. Natl. Acad. Sci. USA **98:**4238–4242.
33. **Lee, J. H., and T. R. Hoover.** 1995. Protein crosslinking studies suggest that *Rhizobium meliloti* C4-dicarboxylic acid transport protein D, a sigma54-dependent transcriptional activator, interacts with sigma54 and the beta subunit of RNA polymerase. Proc. Natl. Acad. Sci. USA **92:**9702–9706.
34. **Lee, S. Y., A. De La Torre, D. Yan, S. Kustu, B. T. Nixon, and D. E. Wemmer.** 2003. Regulation of the transcriptional activator NtrC1: structural studies of the regulatory and AAA+ ATPase domains. Genes Dev. **17:**2552–2563.
35. **Lloyd, L. J., S. E. Jones, G. Jovanovic, P. Gyaneshwar, M. D. Rolfe, A. Thompson, J. C. Hinton, and M. Buck.** 2004. Identification of a new member of the phage shock protein response in *Escherichia coli*, the phage shock protein G (PspG). J. Biol. Chem. **279:**55707–55714.
36. **Lupas, A., M. Van Dyke, and J. Stock.** 1991. Predicting coiled coils from protein sequences. Science. **252:**1162–1164.
37. **Lupas, A.** 1996. Coiled coils: new structures and new functions. Trends Biochem. Sci. **21:**375–382.
38. **Maxson, M. E., and A. J. Darwin.** 2004. Identification of inducers of the *Yersinia enterocolitica* phage shock protein system and comparison to the regulation of the RpoE and Cpx extracytoplasmic stress responses. J. Bacteriol. **186:**4199–4208.
39. **Miller, J. H.** 1992. A short course in molecular genetics. Cold Spring Harbor Laboratory Press, Cold Spring Harbor, N.Y.
40. **Model, P., G. Jovanovic, and J. Dworkin.** 1997. The *Escherichia coli* phage shock protein (*psp*) operon. Mol. Microbiol. **24:**255–261.
41. **Morris, L., W. Cannon, F. Claverie-Martin, S. Austin, and M. Buck.** 1994. DNA distortion and nucleation of local DNA unwinding within sigma54 (sigmaN) holoenzyme closed promoter complexes. J. Biol. Chem. **269:**11563–11571.
42. **Neuwald, A., L. Aravind, J. L. Spouge, and E. V. Koonin.** 1999. AAA+: a class of chaperone-like ATPase associated with the assembly, operation, and disassembly of protein complexes. Genome Res. **9:**27–43.
43. **Nishiyama, K., A. Fukuda, K. Morita, and H. Tokuda.** 1999. Membrane deinsertion of SecA underlying proton motive force-dependent stimulation of protein translocation. EMBO J. **18:**1049–1058.
44. **Polard, P., and M. Chandler.** 1995. An *in vivo* transposase-catalyzed single-stranded DNA circularization reaction. Genes Dev. **9:**2846–2858.
45. **Rappas, M., J. Schumacher, F. Beuron, H. Niwa, P. Bordes, S. R. Wigneshweraraj, C. Keetch, C. Robinson, M. Buck, and X. Zhang.** Unpublished data.
46. **Schumacher, J., X. Zhang, S. Jones, P. Bordes, and M. Buck.** 2004. ATP-dependent transcriptional activation by bacterial PspF AAA+ protein. J. Mol. Biol. **338:**863–875.
47. **Studholme, D. J., and R. Dixon.** 2003. Domain architectures of sigma54-dependent transcriptional activators. J. Bacteriol. **185:**1757–1767.
48. **Wang, Q., J. G. Frye, M. McClelland, and R. M. Harshey.** 2004. Gene expression patterns during swarming in *Salmonella typhimurium*: genes specific to surface growth and putative new motility and pathogenicity genes. Mol. Microbiol. **52:**169–187.
49. **Wang, Y. K., J. H. Lee, J. M. Brewer, and T. R. Hoover.** 1997. A conserved region in the sigma54-dependent activator DctD is involved in both binding to RNA polymerase and coupling ATP hydrolysis to activation. Mol. Microbiol. **26:**373–386.
50. **Westphal, S., L. Heins, J. Soll, and U. C. Vothknecht.** 2001. Vipp1 deletion mutant of *Synechocystis*: a connection between bacterial phage shock and thylakoid biogenesis? Proc. Natl. Acad. Sci. USA **98:**4243–4248.
51. **Xu, H., and T. R. Hoover.** 2001. Transcriptional regulation at a distance in bacteria. Curr. Opin. Microbiol. **4:**138–144.
52. **Zhang, X., A. Shaw, P. A. Bates, R. H. Newman, B. Gowen, E. Orlova, M. A. Gorman, H. Kondo, P. Dokurno, J. Lally, G. Leonard, H. Meyer, M. van Heel, and P. S. Freemont.** 2000. Structure of the AAA ATPase p97. Mol. Cell **6:**1473–1484.
53. **Zhang, X., M. Chaney, S. R. Wigneshweraraj, J. Schumacher, P. Bordes, W. Cannon, and M. Buck.** 2002. Mechanochemical ATPases and transcriptional activation. Mol. Microbiol. **45:**895–903.